Chicxulub impact predates the K-T boundary mass extinction

Gerta Keller*†, Thierry Adatte‡, Wolfgang Stinnesbeck§, Mario Rebolledo-Vieyra¶, Jaime Urrutia Fucugauchi‖, Utz Kramar, and Doris Stüben****

*Department of Geosciences, Princeton University, Princeton, NJ 08540; ‡Institute of Geology, University of Neuchatel, 2007 Neuchatel, Switzerland; §Geological Institute and **Institute for Mineralogy and Geochemistry, University of Karlsruhe, D-76128 Karlsruhe, Germany; ¶Laboratoire des Sciences du Climat et l'Environnement, Unité Mixte de Recherche Centre National de la Recherche Scientifique–Commissariat à l'Energie Atomique, Bât 12, Avenue de la Terrasse, 91198 Gif-sur-Yvette Cedex, France; and ‖Instituto de Geofisica, Universidad Nacional Autonóma de México, Ciudad Universitaria, Mexico City, CP 04510, Mexico

Communicated by W. Jason Morgan, Princeton University, Princeton, NJ, January 20, 2004 (received for review October 3, 2003)

Since the early l990s the Chicxulub crater on Yucatan, Mexico, has been hailed as the smoking gun that proves the hypothesis that an asteroid killed the dinosaurs and caused the mass extinction of many other organisms at the Cretaceous-Tertiary (K-T) boundary 65 million years ago. Here, we report evidence from a previously uninvestigated core, Yaxcopoil-1, drilled within the Chicxulub crater, indicating that this impact predated the K-T boundary by ≈300,000 years and thus did not cause the end-Cretaceous mass extinction as commonly believed. The evidence supporting a pre-K-T age was obtained from Yaxcopoil-1 based on five independent proxies, each with characteristic signals across the K-T transition: sedimentology, biostratigraphy, magnetostratigraphy, stable isotopes, and iridium. These data are consistent with earlier evidence for a late Maastrichtian age of the microtektite deposits in northeastern Mexico.

The search for the K-T impact crater effectively ended in the early l990s with the discoveries of the Chicxulub crater and its estimated diameter between 180 and 280 km (1–4). The impact ejecta (microtektites) in Haiti and northeastern Mexico (5, 6) and melt rock in the Chicxulub cores have similar geochemistry, and the 39Ar/40Ar ages are within ±200,000 years (200 ky) of the K-T boundary (7, 8). These observations made a convincing case for Chicxulub as the long-sought K-T boundary impact crater and cause for the end-Cretaceous mass extinction. But doubts persisted regarding the precise age and size of the impact crater (2–4, 9), the origin of the so-called megatsunami deposits (5, 10–12), and the nature of the mass extinction (13, 14). To resolve these issues, the International Continental Scientific Drilling Program (ICDP) supported the drilling of a new core within the Chicxulub crater (Yaxcopoil-1 drilled between December 2001 and February 2002) with the stated objectives to determine the precise age of the crater and its link to the global K-T boundary layer, to unravel Chicxulub's role in the K-T mass extinction, and to study the cratering event and size of the impact crater (15).

Chicxulub Core Yaxcopoil-1 (Yax-1)

Yax-1 is located 40 km southwest of Merida, Mexico, and ≈60 km from the center of the Chicxulub structure (Fig. 1). A continuous core sequence was recovered from 400 to 1,511 m below the surface (15).[†††‡‡] Between 794.65 and 894 m, a 100-m-thick impact (suevite) breccia overlies a 617-m-thick sequence of horizontally layered shallow-water lagoonal to subtidal Cretaceous limestones, dolomites, and anhydrites. The first 85 m of the impact (suevite) breccia consist primarily of clasts from these underlying shallow-water lithologies, some crystalline rocks of continental basement origin, and devitrified glass (Cheto smectite) fragments and spherules.[††] The upper 15 m of the breccia are stratified with alternating layers of upward fining clasts (3–5 cm at the base to 2–5 mm at the top), coarse cross-bedding structures, and gray friable sand layers in the top meter, all of which indicate reworking and high-energy current transport after deposition of the impact (suevite) breccia.

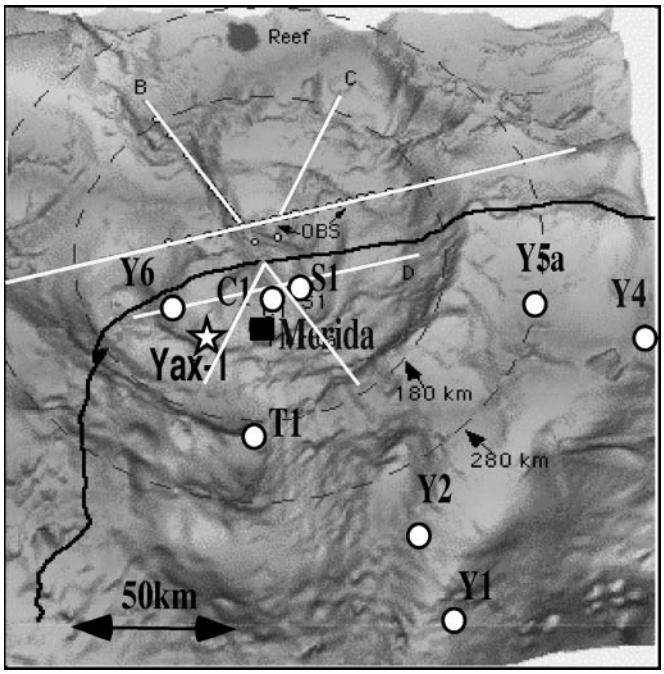

Fig. 1. Location of core Yax-1 and other Yucatan cores relative to seismic lines and the proposed crater size superimposed over the gravimetric anomaly map.

Above the suevite breccia, with a disconformity separating the two, are 50 cm of finely laminated dolomitic and micritic limestones that contain Late Maastrichtian microfossils. A glauconitic clay (16) above this 50-cm-thick interval can be identified as the K-T boundary based on the presence of early Danian microfossils in the overlying strata.

Consequently, the suevite breccia that marks the Chicxulub impact is within Late Maastrichtian sediments and below the K-T boundary. This suggests two possibilities: (*i*) the sediments between the breccia and the K-T boundary were deposited as backwash and crater infill after the impact event, or (*ii*) the Chicxulub impact predates the K-T boundary and hence was not

Abbreviations: K-T, Cretaceous-Tertiary; ky, thousand years; XRD, x-ray diffraction; Yax-1, Yaxcopoil-1.

†To whom correspondence should be addressed. E-mail: gkeller@princeton.edu.

††Stinnesbeck, W., Keller, G., Adatte, T. & Stueben, D. (2003) *Geophys. Res. Abstr.* **5,** 10868.

‡‡Smit, J., Dressler, B. O., Buffler, R., Moran, D., Sharpton, V. L., Stoeffler, D., Urrutia, J. & Morgan, J. (2003) *Geophys. Res. Abstr.* **5,** 06498.

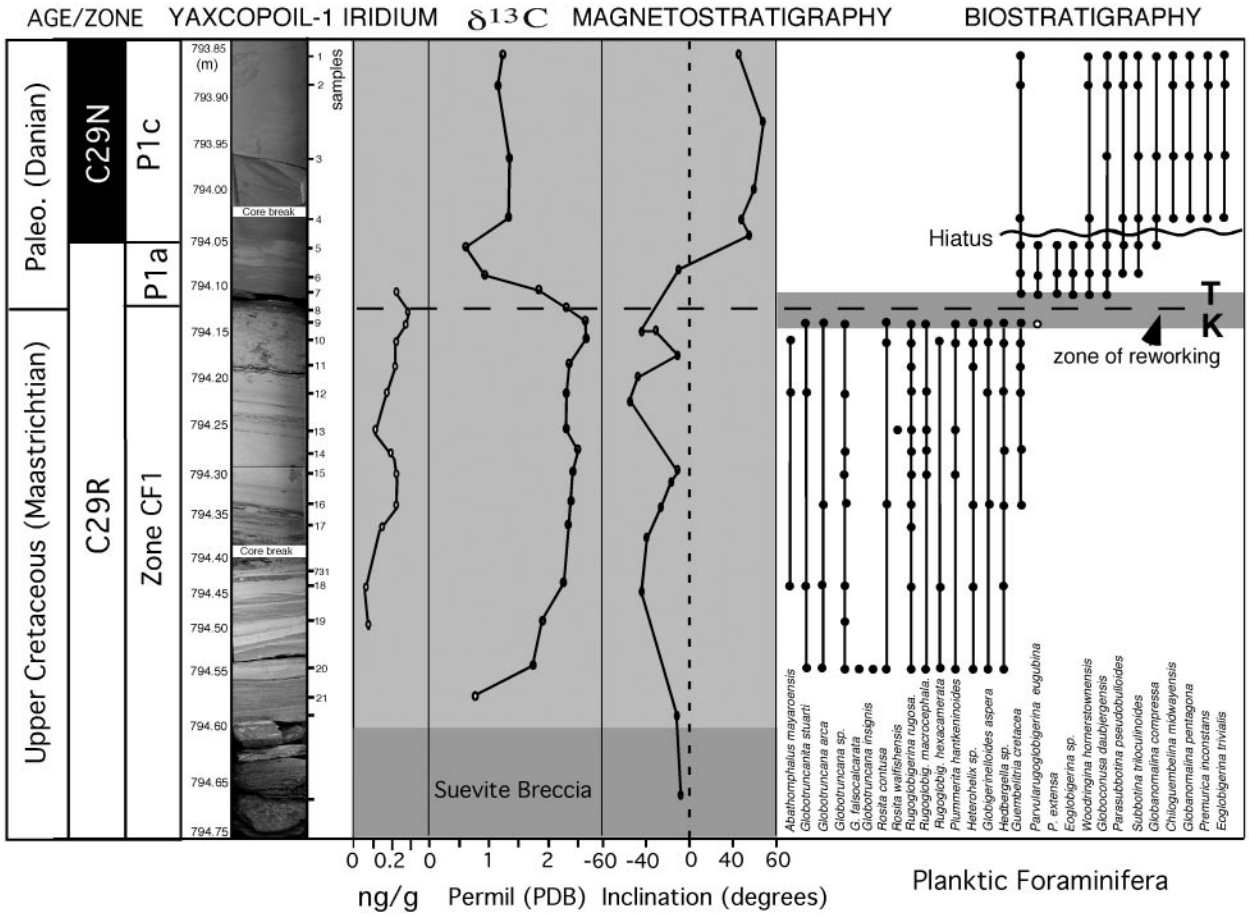

Fig. 2. Five sediment and age-related proxies reveal Late Maastrichtian pelagic sediments overlying the impact breccia in the Chicxulub core Yax-1. Note that zones P0, most of Pla, and probably the uppermost part of zone CF1 are missing. In addition, the hiatus at 794.05 m marks the loss of zone Plb and the lower part of Plc. The absence of the Ir anomaly is likely due to the hiatus that spans the K-T boundary.

the cause of the end-Cretaceous mass extinction as commonly believed.

To determine the age of the Chicxulub impact and the nature of sediment deposition we studied this critical core interval from the top of the impact breccia to the Early Tertiary (794.65–793.85 m) at high resolution (2- to 5-cm sample spacing) and with all available methods, including sedimentology, clay minerals [x-ray diffraction (XRD) and environmental scanning electron microscope analyses], microfossils (thin sections), magnetostratigraphy, stable isotopes (bulk carbonate), and iridium (instrumental neutron activation analysis) analyses. Four samples within the breccia (at 827.81, 851,02, 861.74, and 876.37 m) were analyzed for comparison with the overlying strata.

Age of Chicxulub Impact

K-T Boundary. The K-T boundary is identified at 794.11 m, ≈50 cm above the impact breccia (Fig. 2). The boundary is characterized by a 2- to 3-cm-hick dark gray-green marly limestone with a 3- to 4-mm-thick green glauconitic clay (17) that marks an erosional disconformity. The 50-cm interval below the K-T boundary is in reversed polarity C29r. It is clear that 7 cm above the K-T boundary the core is normally magnetized (in chron 29n). The change appears to occur more than 4 cm above the K-T boundary, although only one data point occurs. Stable carbon isotopes show the high $\delta^{13}C$ values of the Late Maastrichtian above the breccia, followed by the characteristic negative excursion at the K-T boundary. (The low value in the dolomite sample 21 is due to diagenetic effects.) Iridium concentrations are within the range of background values and only reach 0.29 ng/g at the K-T boundary (Fig. 2). The absence of an Ir anomaly and the short interval of C29r above the K-T boundary suggest a hiatus, as also indicated by biostratigraphy.

The First Tertiary (Danian) planktic foraminifera are present 2 cm above the K-T boundary green clay and disconformity and indicate zone Pla (e.g., *Parvularugoglobigerina eugubina*, *Parvulaugoglobigerina extensa*, *Eoglobigerina* sp., *Woodringina hornerstownensis*, and *Globoconusa daubjergensis*, plus rare reworked Cretaceous species). In the overlying mottled, bioturbated 5-cm interval (samples 5 and 6), these early Danian species are common, along with well developed *Parasubbotina pseudobulloides*, *Subbotina triloculinoides*, and *Globanomalina compressa*, which are characteristic of an upper Pla assemblage and suggests that the earliest Danian interval (zones P0 and lower Pla) is missing.

The missing interval at the K-T boundary can be estimated from planktic foraminiferal assemblages and magnetostratigraphy. Early Danian zones P0 and Pla are correlative with C29r above the K-T boundary, which spans about the first 275 ky of the Tertiary (19, 20). At Yax-1 this interval is represented by only 6 cm of the upper zone Pla and C29r, indicating >250 ky missing and probably part of the uppermost Maastrichtian. This may explain the absence of the characteristic Ir anomaly that marks the K-T boundary worldwide.

In the marly limestone at 6 cm above the K-T boundary, another abrupt change occurs in the species assemblage to larger size, along with the abrupt appearance of the upper zone Plc (2)

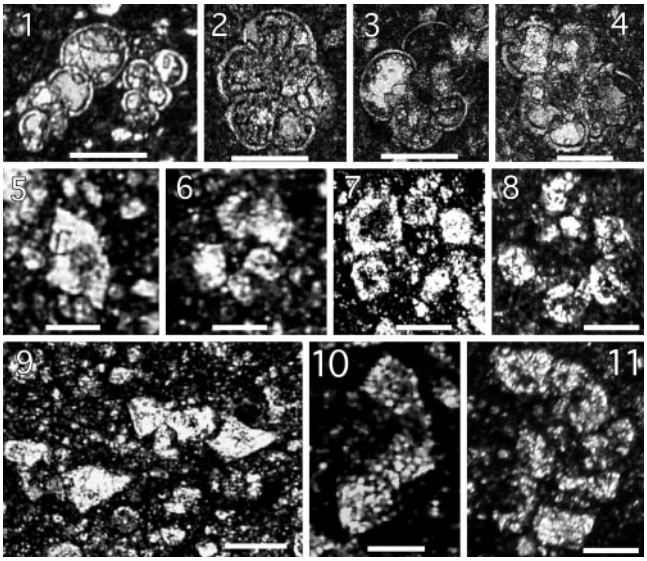

Fig. 3. Thin-section micrographs of Late Maastrichtian and Early Paleocene planktic foraminifera from Yax-1. (Scale bar = 100 μm for images 1–3; fscale bar = 200 μm for images 4–11.) Early Paleocene zones Pla-Plc: image 1, *W. hornerstownensis* (sample 1); image 2, *P. eugubina* (sample 6); image 3, *P. pseudobulloides* (sample 5); image 4, *P. inconstans* (sample 4). Late Maastrichtian Zone CF1: image 5, *Plummerita hantkeninoides* (sample 20); image 6, *Rugoglobigerina macrocephala* (sample 9); images 7 and 8, *Rugoglobigerina rugosa* (samples 19 and 12); image 9, *Globotruncana insignis* (sample 20); image 10, *Globotruncana arca* (sample 9); image 11, *Rosita contusa* (sample 9).

assemblage (e.g., absence of *P. eugubina* and presence of *Premurica inconstans*, *Eoglobigerina trivialis*, and *Globanomalina pentagona*). This marks another major hiatus (794.05 m) with zone Plb and the lower part of zone Plc(l) missing, as also indicated by the magnetic polarity change from C29r to C29n.

K-T and early Danian hiatuses of these magnitudes have been observed throughout the Caribbean and Gulf of Mexico (21) and in the deep sea globally (20) and may be linked to intensified deep-water currents during the Early Paleocene.

Age of Unit Between Breccia and K-T. Planktic foraminifera within the 50-cm-thick laminated dolomitic and micritic limestones between the breccia and K-T boundary provide critical age constraints for deposition of this unit in addition to magnetostratigraphy. Examination of thin sections reveal the laminated intervals to be rich in Late Maastrichtian planktic foraminifera, although they are invariably recrystallized and poorly preserved in these micritic limestones. The recrystallization process, however, retained the species morphology and the lighter colored shell calcite relative to the surrounding micrite, although the images at very high magnification show the crystalline micrite texture. For this reason, magnification of species is limited ($\times$100–200) and the images are often fuzzy (Fig. 3). We show representative species from various intervals at a magnification that still permits recognition of characteristic species morphologies. To illustrate that these forms are foraminifera and to differentiate them from crystalline sediments, we show them embedded in the darker surrounding micritic limestone. No foraminifera are preserved in the dolomitic layers (e.g., sample 21) characterized by dolomite rhombs.

Diverse and abundant planktic foraminiferal assemblages are present in all laminated micritic limestone samples, although benthic foraminifera are less common (mostly buliminellids). The planktic assemblages consist of characteristic Late Maastrichtian zone CF1 species, including *Globotruncanita stuarti*, *G. insignis, G. arca*, *Globotruncanita falsocalcarata*, *Abathomphalus mayaroensis*, *R. contusa, Rosita walfishensis, R. rugosa*, *R. macrocephala*, *P. hantkeninoides*, *Globotruncanella petaloidea*, *Heterohelix*, *Hedbergella* sp., and *Globigerinelloides aspera* (Figs. 2 and 3). Zone CF1 spans the last 300 ky of the Cretaceous, correlative with the upper part of magnetochron C29r below the K-T boundary. These zone CF1 assemblages therefore indicate that deposition of the 50 cm of laminated micritic limestones occurred after the Chicxulub impact and before the K-T boundary mass extinction.

Alternatively, could the 50-cm-thick laminated micritic limestones and Late Maastrichtian foraminifera represent reworking by backwash and crater infill after deposition of the impact breccia? Microfossil evidence suggests that this is not the case for several reasons.

1. Backwash and crater infill requires high-energy currents to erode and transport material, including diverse clasts and faunal elements from the impact breccia and the underlying lithologies and their shallow-water benthic foraminifera. No evidence for such reworking exists in the critical 50 cm between the breccia unit and the K-T boundary, nor does sedimentary evidence exist for a high-energy depositional environment (see below).
2. Before the impact, the Yucatan shelf in the Chicxulub area was a shallow subtidal environment that did not support planktic foraminiferal assemblages. After the impact these microfossils are abundantly present. If they were eroded and transported over great distances from the open ocean (e.g., backwash), the evidence of high-energy sedimentary structures and of diverse clasts and diverse species from various older age intervals should be clear. No evidence for any of the above exists.
3. Planktic foraminiferal assemblages within the 50-cm interval are of high diversity with small and large, thin- and thick-shelled species, and all are characteristic of the latest Maastrichtian zone CF1 age. Such uniform assemblages, and the absence of older reworked species, cannot be explained by backwash and crater infill, but they are consistent with *in situ* deposition in a low-energy hemipelagic environment.
4. The presence of burrows below the K-T boundary and in the four glauconitic layers within the 50-cm interval below indicates that deposition occurred in a normal sedimentary environment with burrowing organisms on the ocean floor. If these deposits consisted of high-energy backwash and current reworking, burrows could not have been preserved.

The evidence thus indicates that the Late Maastrichtian planktic foraminiferal assemblages were deposited *in situ* after the impact event in a low-energy hemipelagic environment that was deep enough ($\approx$100 m) to support planktic foraminifera and supported active, burrowing benthic communities. The deepening may have been caused by the crater excavation and the sea level rise during the latest Maastrichtian. This interpretation can be further tested based on the nature of sediment deposition.

Depositional Environment. The nature and depositional environment of the 50-cm interval between the disconformities at the top of the impact breccia and the K-T boundary provides another critical test of *in situ* versus backwash deposition and hence the age of the impact, whether K-T or pre-K-T. The 50-cm interval consists predominantly of laminated micritic limestones with microlayers or patches of anhedral dolomite crystals and a 5-cm-thick dolomite layer at the base (Fig. 4). The micritic limestones indicate deposition under low-energy, quiet water conditions, whereas the dolomite formed by diagenetic replacement of the precursor limestone with the original laminated texture is still visible.

Sedimentary structures indicate a variable depositional history. Five thin green clayey microclast layers are embedded in

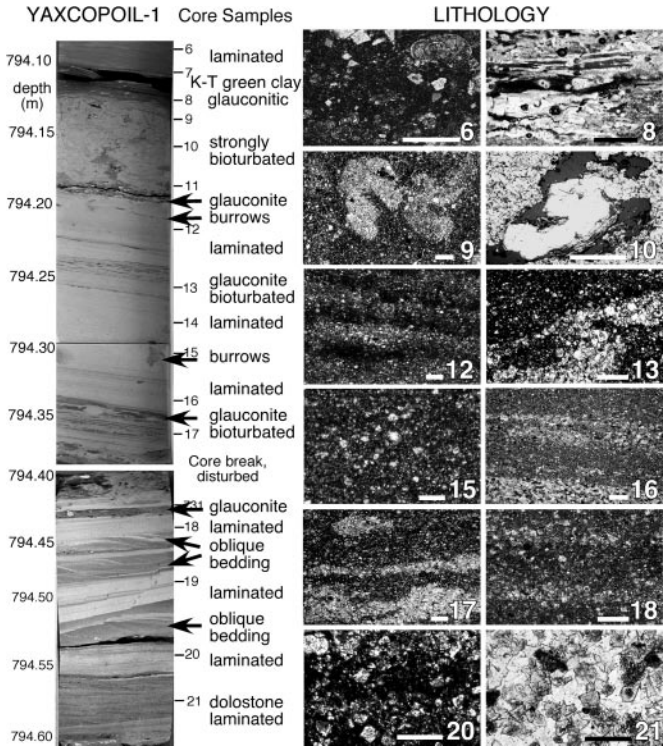

Fig. 4. Litholog of the 50-cm interval between the disconformities at the top of the breccia and the K-T boundary. (Scale bar = 0.1 mm for samples 6 and 8 and 1 mm for samples 1–5, 7, and 9–21.) Sedimentary features of most sample intervals are shown in thin-section micrographs with numbers keyed to the sample location in the litholog. Note the four distinct green microlayers (<1 cm), each with glauconite and/or glauconite-coated microclasts (see Fig. 5).

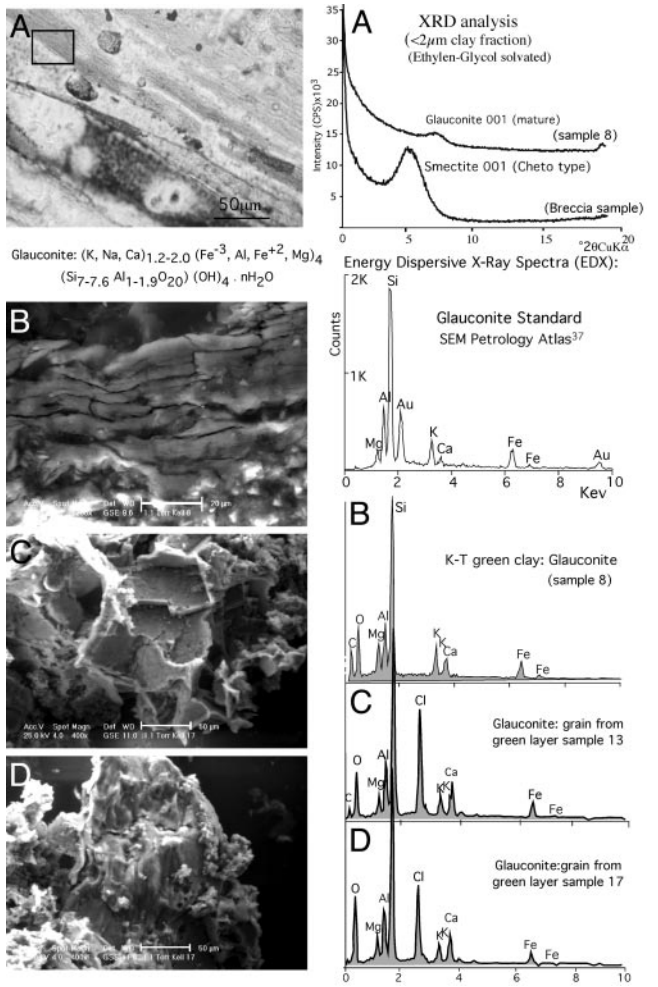

Fig. 5. (*A*) Thin-section micrograph of the green K-T clay layer (sample 8) with insert marking location of analysis. The XRD diffractogram of this green clay indicates the presence of mature glauconite (17). In contrast, XRD analysis of breccia samples shows the presence of well crystallized Cheto smectite, which is a typical altered glass product. (*B*) Environmental scanning electron microscope micrograph of the K-T green clay (sample 8) with electron diffractometer x-ray analysis that indicates a glauconitic composition (shaded interval). *C* and *D* show similar glauconitic compositions for insoluble residue grains from the green layers of samples 13 and 17. (Note that the Cl peak is due to the chlorhydric acid used in preparation of insoluble residues.) The glauconite reference standard from the SEM Petrology Atlas (18) is shown for comparison.

laminated limestones at 794.43, 794.34–794.35, 794.24, 794.19, and 794.11 m; the latter marks the K-T boundary (Fig. 4). The insoluble residues of these intervals reveal that the microclasts are of glauconite origin and/or have *in situ* glauconite coating. environmental scanning electron microscope and XRD analyses of microclasts and the green clay reveal a glauconite XRD pattern (17) (Fig. 5) with no altered glass present. For comparison, we have analyzed four samples from the breccia at depths of 827.81, 851.02, 861.74, and 876.37 m. XRD analyses of these breccia intervals show the presence of Cheto smectite, which is characteristic of altered glass (22) (Fig. 5*A*). Glauconite forms at the sediment–water interface in environments with very slow detritus accumulation. The five microclast and green clay layers therefore indicate long pauses in the overall quiet depositional environment with reduced sedimentation and the formation of glauconite followed by sediment winnowing, clast generation, and small-scale transport by minor current activity.

Glass is very rare in the entire 50-cm interval. No breccia clasts were observed. Bioturbation is common in and around the microclast layers at 794.19, 794.24, and 794.34 m, and the interval below the K-T is strongly burrowed by invertebrates, some of which may have penetrated to form the larger isolated burrow at 794.31 m (Fig. 4). This finding suggests that an active benthic community thrived on the ocean floor during sediment deposition and argues against rapid deposition by backwash.

The change in the dip angle between 794.34 and 794.52 m may be due to compaction/settling of the underlying ejecta material that locally changed the seabed slope. The tiny extensional syn-sedimentary growth faults around 794.50 m may also have been caused by this process.

In the lower part of the 50-cm interval, the oblique bedding in three thin (1-cm) layers between 794.45 and 794.53 m may have been formed by slightly agitated waters. However, the absence of grain-size changes suggests that this could be a diagenetic feature. Sediments at the core break (794.40 m) are mechanically disturbed by drilling, but their gray-green color suggests a glauconite component as in the green layers above and below.

Sedimentology of the 50-cm interval overlying the suevite breccia thus indicates that the postimpact deposition occurred in a low-energy environment with little current activity, which favored deposition of laminated limestones. But this environment was interrupted four times for prolonged times with slightly more active winnowing activity before the K-T boundary and again at the boundary, which was probably related to changes in sea level. Each time, sedimentation was reduced, allowing the formation of glauconite, which was then followed by sediment winnowing, clast generation, and transport before the return of low-energy laminated sediment deposition.

The scarcity of glass or breccia clasts in these sediments, the

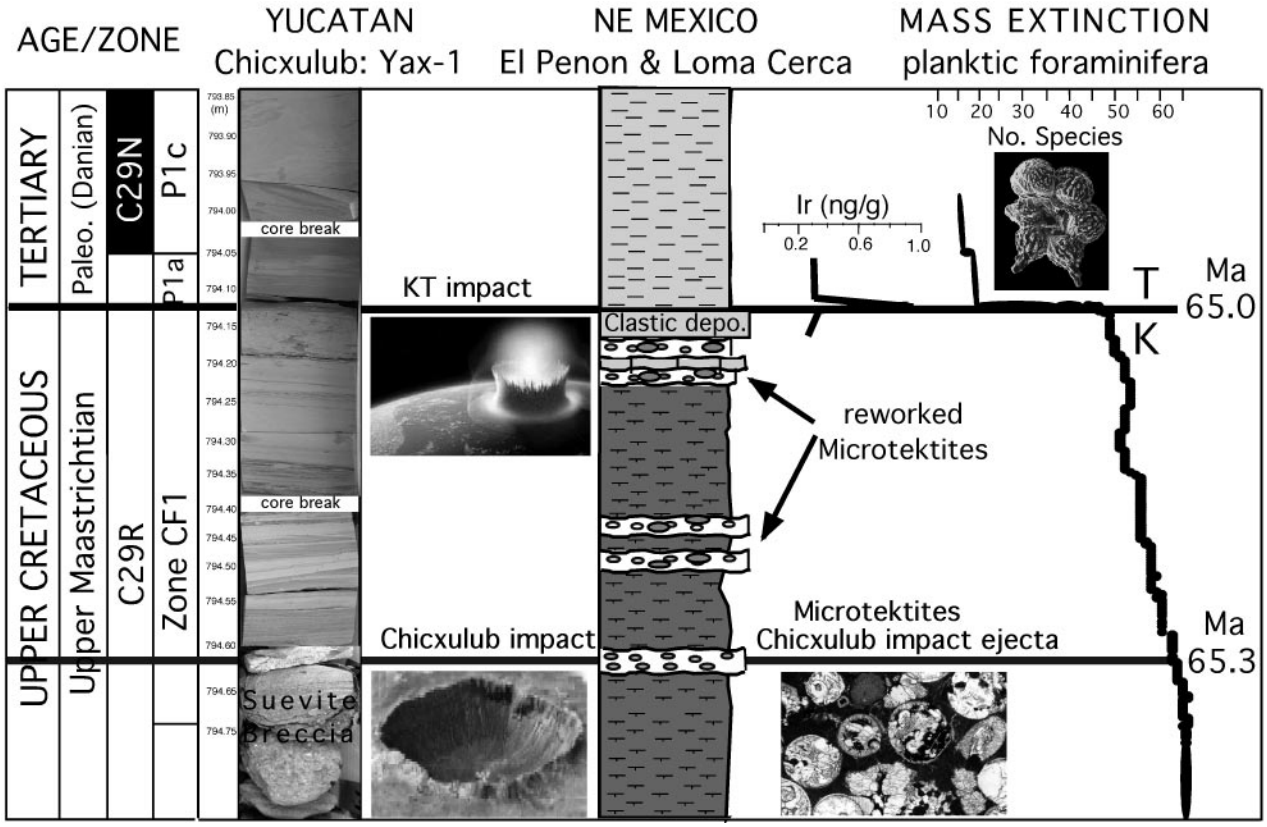

Fig. 6. Proposed correlation of Chicxulub impact breccia in core Yax-1 with the oldest microtektite layer in Late Maastrichtian marls of the Mendez Formation at El Penon and Loma Cerca in northeastern Mexico (22, 24). (We consider the younger microtektite layers that are interbedded in marls to be reworked.) The Ir anomaly in northeastern Mexico is at the K-T boundary.

low-energy environment, and the repeated pauses and formation of glauconite provide no evidence for rapid deposition related to backwash and crater infill for this 50-cm-thick interval.

Pre-K-T Age of Chicxulub Impact. The age of the Chicxulub impact can now be determined from the Yax-1 core based on the stratigraphic position of the breccia relative to the K-T boundary, the nature of sediment deposition between the breccia and the K-T boundary, and the age of the planktic foraminiferal assemblages within these sediments. At Yax-1 the top of the breccia is marked by a disconformity and the K-T boundary is marked by a green glauconitic clay that forms another disconformity. In between are 50 cm of laminated dolomitic and micritic limestones interrupted by four glauconitic horizons. These sediments indicate a quiet hemipelagic environment, interrupted at times by slightly increased current activity that resulted in reduced sediment deposition, winnowing, and short-distance transport. Bioturbation at these horizons and the K-T boundary indicate an ocean floor colonized by invertebrates.

The planktic foraminiferal assemblages within these sediments are characteristic of zone CF1, which spans the last 300 ky of the Maastrichtian. Magnetostratigraphy indicates C29r below the K-T boundary, which spans the last 570 ky of the Maastrichtian. Also, the $\delta^{13}C$ values are characteristic of the Late Maastrichtian. All three age proxies are thus consistent with a pre-K-T age for the underlying impact breccia, whereas the sedimentology rules out backwash and crater infill for the 50-cm interval between the breccia and K-T boundary. Based on these data, the Chicxulub impact predates the K-T boundary and occurred sometime during the early part of zone CF1 and the middle part of C29r below the K-T boundary.

Other Evidence of Pre-K-T Age. The pre-K-T age determined from Yax-1 adds to the accumulating evidence of a pre-K-T age for the Chicxulub impact in northeastern Mexico, where impact ejecta layers (microtektites) have been discovered interbedded in Late Maastrichtian marls in numerous localities (23). At El Peñon and 25 km northeast at Loma Cerca four microtektite layers are interbedded in 10 m of pelagic marls, with no evidence of folding or faulting. Planktic foraminifera indicate that deposition occurred during the late Maastrichtian zone CF1 with the oldest layer near the base of the zone (23, 24) (Fig. 6). We consider the lowermost microtektite layer as the original ejecta from the Chicxulub impact, whereas the upper layers appear to be repeatedly reworked by currents, as indicated by common marl clasts and shallow-water benthic foraminifera and debris. Based on biostratigraphy and sediment accumulation rates, the oldest microtektite layer at these Mexican sites was deposited ≈300 ky before the K-T boundary, which also suggests that the Chicuxulub impact predates the K-T boundary.

A pre-K-T age for the Chicxulub impact was first suggested by Lopez Ramos (25) based on abundant late Maastrichtian planktic foraminifera in marls and limestones above the impact breccia of PEMEX well C1 located near the center of the Chicxulub crater (Fig. 1). This Late Maastrichtian unit overlying the impact breccia was also identified by Ward *et al.* (9) in well Sacapuc-1 based on electric log correlations and determined to be ≈18 m thick. To date biostratigraphic, magnetostratigraphic, stable isotope, or iridium data do not support a K-T boundary age for the Chicxulub impact.

Multiple Impacts and Mass Extinction

The pre-K-T age of the Chicxulub impact lends support to a multiple-impact scenario with impacts during the Late Maas-

trichtian, at ≈300 ky before the K-T boundary and at the K-T boundary (Fig. 6). During the Late Maastrichtian in the North Sea (Silverpit crater) (26) and Ukraine (Boltysh crater) (27), evidence of smaller impact craters also exist. In addition, Late Maastrichtian Ir and PGE anomalies have been reported from Oman (28). Another impact may have occurred in the early Danian (*P. eugubina* zone, ≈64.9 million years ago) as suggested by Ir and PGE anomaly patterns in sections from Mexico, Guatemala, and Haiti (24, 29, 30).

The Late Maastrichtian Chicxulub impact coincided with major Deccan volcanism (31, 32), greenhouse warming (65.4–65.2 million years ago) (33), and a gradual decrease in species diversity during the last 700 ky before the K-T boundary, but no major species extinctions (11, 34) (Fig. 6). However, a shift to ecological generalist dominated assemblages in planktic foraminifera, reflecting major biotic stress associated with these Late Maastrichtian environmental changes, although the biotic stress appears to be primarily due to major volcanism (35). The mass extinction coincided with the K-T boundary impact and Deccan volcanism and eliminated all tropical and subtropical species, all of which were rare by that time with a combined relative abundance averaging <15% of the total foraminiferal population (13). This finding suggests that the K-T boundary impact (and volcanism) may have been the straw that broke the camel's back, rather than the catastrophic kill of a healthy thriving community.

With mounting evidence for a pre-K-T age for the Chicxulub impact from microtektite layers in northeastern Mexico (23, 24), Chicxulub core Yax-1, and earlier wells C1 and Sacapuc-1 (9, 25), the location of the K-T impact crater remains unknown. The Shiva crater in India has been proposed as a possible candidate (36). Biotic effects of large impacts need to be reevaluated, in particular, those associated with the Late Maastrichtian Chicxulub impact, and differentiated from biotic effects caused by Deccan volcanism and greenhouse warming.

We thank Jason Morgan for his suggestions, support, and sponsorship; the reviewers Paul Wignall, Juergen Remane, and Valeria Luciani for critical comments and suggestions; Hedi Oberhänsli, Sigal Abramovich, Isabella Premoli Silva, and Bilal Haq for their expert opinions on identifying Late Cretaceous foraminifera; A. Villard for ultrapolished thin section preparation; and M. Dadras (Institut de Microtechnique, Neuchâtel, Switzerland) for environmental scanning electron microscope analyses. This study was supported by National Science Foundation Grant EAR-0207407 (to G.K.), German Science Foundation Grants STI 128/7-1 to -3 and STU 169/22-3, and Swiss National Fund nos. 8220-028367 and 21-67702.02. M.R.-V. received a postdoctoral grant from Consejo Nacional de Ciencia y Technología (Mexico) and le Laboratoire des Sciences du Climat et l'Environnement, Centre National de la Recherche Scientifique-Commissariat à l'Energie Atomique, France.

1. Alvarez, L. W., Alvarez, W., Asaro, F. & Michel, H. V. (1980) *Science* **208,** 1095–1108.
2. Hildebrand, A. R., Penfield, G. T., Kring, D. A., Pilkington, M., Camargo, Z. A., Jacobson, S. & Boynton, W. V. (1991) *Geology* **19,** 867–871.
3. Sharpton, V. L., Dalrymple, G. B., Marin, L. E., Ryder, G., Schuraytz, B. C. and Urrutia-Fucugauchi, J. (1992) *Nature* **359,** 819–820.
4. Urrutia Fucugauchi, J., Marín, L. & Trejo-García, A. (1996) *Geophys. Res. Lett.* **23,** 1565–1568.
5. Smit, J., Montanari, A., Swinburne, N. H. M., Alvarez, W., Hildebrand, A., Margolis, S. V., Claeys, P., Lowrie, W. & Asaro, F. (1992) *Geology* **20,** 99–104.
6. Izett, G. A. (1991) *J. Geophys. Res.* **96,** 20879–20905.
7. Sigurdsson, H., Bonte, T., Turpin, L., Steinberg, M., Pradel, P., Jehanno, C. & Rocchia, R. (1991) *Nature* **353,** 482–487.
8. Swisher, C. C., Grajales-Nishimura, J. M., Montanari, A., Margolis, V., Claeys, P., Alvarez, W., Renne, P., Cedillo-Pardo, E., Maurasse, F. J. M., Curtis, G. H., *et al.* (1992) *Science* **257,** 954–958.
9. Ward, W., Keller, G., Stinnesbeck, W. & Adatte, T. (1995) *Geology* **23,** 873–876.
10. Stinnesbeck, W., Barbarin, J. M., Keller, G., Lopez-Oliva, G., Pivnik, D. A., Lyons, J. B., Officer, C. B., Adatte, T., Graup, G., Rocchia, R. & Robin, E. (1993) *Geology* **21,** 797–800.
11. Keller, G., Lopez-Oliva, J. G., Stinnesbeck, W. & Adatte, T. (1997) *Geol. Soc. Am. Bull.* **109,** 410–428.
12. Ekdale, A. A. & Stinnesbeck, W. (1998) *Palaios* **13,** 593–602.
13. Keller, G. (2001) *Planet. Space Sci.* **49,** 817–830.
14. MacLeod, N., Rawson, P. F., Forey, P. L., Banner, F. T., Boudagher-Fadel, M. K., Bown, P. R., Burnett, J. A., Chambers, P., Culver, S., Evans, S. E., *et al.* (1997) *J. Geol. Soc. (London)* **154,** 265–292.
15. Dressler, B. O., Sharpton, V. L., Morgan, J., Buffler, R., Moran, D., Smit, J., Stoeffler, D. & Urrutia, J. (2003) *EOS Trans. Am. Geophys. Union* **84,** 125.
16. Odin, G. S. (1975) Ph.D. thesis (Pierre et Marie Curie University, Paris).
17. Chamley, H. (1989) *Clay Sedimentology* (Springer, Berlin) pp. 222–226.
18. Welton, E. J. (1984) in *SEM Petrology Atlas*, The AAPG Methods in Exploration Series, ed. Steinmetz, R. (American Association of Petroleum Geologists, Tulsa, OK), Vol. 4.
19. Berggren, W. A., Kent, D. V., Swisher, C. C. & Aubry, M. P. (1995) *Spec. Pub.-Soc. Econ. Paleontol. Mineral.* **54,** 129–212.
20. MacLeod, N. & Keller, G. (1991) *Geology* **19,** 497–501.
21. Keller, G., Lyons, J. B., MacLeod, N. & Officer, C. B. (1993) *Geology* **21,** 776–780.
22. Keller, G., Stinnesbeck, W., Adatte, T., Holland, B., Stueben, D., Harting, M. DeLeon, C. & J. De la Cruz. (2003) *J. Geol. Soc. (London)* **160,** 1–13.
23. Keller, G., Stinnesbeck, W., Adatte, T. & Stueben, D. (2003) *Earth-Sci. Rev.* **1283,** 1–37.
24. Keller, G., Adatte, T., Stinnesbeck, W., Affolter, M., Schilli, L. & Lopez-Oliva, J. G. (2002) *Geol. Soc. Am. Spec. Pap.* **356,** 145–161.
25. Lopez Ramos, E. (1975) in *The Gulf of Mexico and the Caribbean*, eds. Nairn, A. E. M. & Stehli, F. G. (Plenum, New York), Vol. 3, pp. 257–282.
26. Stewart, A. S. & Allen, P. J. (2002) *Nature* **418,** 520–521.
27. Kelley, S. P. & Gurov, E. B. (2002) *Meteor. Planet. Sci.* **37,** 1031–1043.
28. Ellwood, B. B., MacDonald, W. D., Wheeler, C. & Benoist, S. L. (2003) *Earth Planet. Sci. Lett.* **206,** 529–540.
29. Stueben, D., Kramar, U., Berner, Z., Eckhardt, J. D., Stinnesbeck, W., Keller, G., Adatte, T. & Heide, K. (2002) *Geol. Soc. Am. Special Pap.* **356,** 163–188.
30. Stinnesbeck, W., Keller, G., Schulte, P. Stueben, D., Berner, Z., Kramar, U. & Lopez-Oliva, J. G. (2002) *J. South Am. Res.* **15,** 497–509.
31. Hoffmann, C., Feraud, G. & Courtillot, V. (2000) *Earth Planet. Sci. Lett.* **180,** 13–27.
32. Courtillot, V., Gallet, Y., Rocchia, R., Feraud, G., Robin, E., Hofmann, C., Bhandari, N. & Ghevariya, Z. G. (2000) *Earth Planet. Sci. Lett.* **182,** 137–156.
33. Li, L. & Keller, G. (1998) *Geology* **26,** 995–998.
34. Abramovich, S. & Keller, G. (2002) *Paleogeogr. Paleoclimatol. Paleoecol.* **173,** 145–164.
35. Keller, G. (2003) *Earth Planet. Sci. Lett.* **215,** 249–264.
36. Chatterjee, S. (1997) in *Proceedings of the 30th International Geological Congress*, eds. Nang, H., Branagan, D. F., Ouyang, Z. & Wang, X. (Geological) Congress, International Science Publishers, The Netherlands), Vol. 26, pp. 31–54.